Molecular basis of cell and developmental biology:

Role of Scarf and Its Binding Target Proteins in Epidermal Calcium Homeostasis

Joonsung Hwang, Alexandr Kalinin, Meeyul Hwang, D. Eric Anderson, Min Jung Kim, Olivera Stojadinovic, Marjana Tomic-Canic, Seung Hun Lee and Maria I. Morasso

J. Biol. Chem. 2007, 282:18645-18653.
doi: 10.1074/jbc.M702035200 originally published online April 30, 2007

THE JOURNAL OF BIOLOGICAL CHEMISTRY VOL. 282, NO. 25, pp. 18645–18653, June 22, 2007
Printed in the U.S.A.

Role of Scarf and Its Binding Target Proteins in Epidermal Calcium Homeostasis*

Received for publication, March 8, 2007, and in revised form, April 16, 2007 Published, JBC Papers in Press, April 30, 2007, DOI 10.1074/jbc.M702035200

Joonsung Hwang[‡], Alexandr Kalinin[‡], Meeyul Hwang[‡], D. Eric Anderson[§], Min Jung Kim[¶], Olivera Stojadinovic[‖], Marjana Tomic-Canic[‖], Seung Hun Lee[¶], and Maria I. Morasso[‡1]

From the [‡]Developmental Skin Biology Unit, NIAMS, and [§]Proteomics and Mass Spectrometry Facility, NIDDK, National Institutes of Health, Bethesda, Maryland 20892, [¶]Department of Dermatology, Yonsei University College of Medicine, Seoul 135-720, Korea, and [‖]Department of Dermatology, Weill Medical College of Cornell University, Hospital for Special Surgery, New York, New York 10021

The novel Ca^{2+}-binding protein, Scarf (skin calmodulin-related factor) belongs to the calmodulin-like protein family and is expressed in the differentiated layers of the epidermis. To determine the roles of Scarf during stratification, we set out to identify the binding target proteins by affinity chromatography and subsequent analysis by mass spectrometry. Several binding factors, including 14-3-3s, annexins, calreticulin, ERp72 (endoplasmic reticulum protein 72), and nucleolin, were identified, and their interactions with Scarf were corroborated by co-immunoprecipitation and co-localization analyses. To further understand the functions of Scarf in epidermis *in vivo*, we altered the epidermal Ca^{2+} gradient by acute barrier disruption. The change in the expression levels of Scarf and its binding target proteins were determined by immunohistochemistry and Western blot analysis. The expression of Scarf, annexins, calreticulin, and ERp72 were up-regulated by Ca^{2+} gradient disruption, whereas the expression of 14-3-3s and nucleolin was reduced. Because annexins, calreticulin, and ERp72 have been implicated in Ca^{2+}-induced cellular trafficking, including the secretion of lamellar bodies and Ca^{2+} homeostasis, we propose that the interaction of Scarf with these proteins might be crucial in the process of barrier restoration. On the other hand, down-regulation of 14-3-3s and nucleolin is potentially involved in the process of keratinocyte differentiation and growth inhibition. The calcium-dependent localization and up-regulation of Scarf and its binding target proteins were studied in mouse keratinocytes treated with ionomycin and during the wound-healing process. We found increased expression and nuclear presence of Scarf in the epidermis of the wound edge 4 and 7 days post-wounding, entailing the role of Scarf in barrier restoration. Our results suggest that Scarf plays a critical role as a Ca^{2+} sensor, potentially regulating the function of its binding target proteins in a Ca^{2+}-dependent manner in the process of restoration of epidermal Ca^{2+} gradient as well as during epidermal barrier formation.

Calcium (Ca^{2+}) is a ubiquitous intracellular messenger that influences numerous cellular processes, such as proliferation, development, and muscle contraction among others. Epidermal differentiation is one of the Ca^{2+}-dependent processes. Mouse keratinocytes cultured in low Ca^{2+} medium (0.05 mM) proliferate repeatedly, but do not differentiate unless the Ca^{2+} concentration exceeds 0.1 mM (1–3). Upon the change into the higher Ca^{2+} concentration, the cultured keratinocytes stop proliferating and begin to differentiate. *In vivo*, an endogenous Ca^{2+} gradient is present in the epidermis of neonatal and adult hairless mice (4). It has been proposed that changes in intracellular Ca^{2+} concentration, which result from both the intercellular Ca^{2+} accumulation in the mid granular layers and Ca^{2+} influx from the upper granular layers, regulate epidermal differentiation. Acute disruption of epidermal permeability by either repeated tape stripping or acetone treatment can alter this Ca^{2+} gradient in the skin (5). The responses following skin barrier disruption involve: a loss of Ca^{2+} from the outer epidermis (stratum granulosum) (6), rapid secretion of lamellar bodies from the outermost granular layers (7) and increased lipid and DNA synthesis (8–11). The Ca^{2+} concentration in the outer layers of the epidermis decreases 3 h after disruption and is restored after 6–24 h (12).

Mechanisms that lead to an increase in intracellular Ca^{2+} concentration include the release of Ca^{2+} from intracellular storages, such as endoplasmic reticulum (ER)[2] or sarcoplasmic reticulum in muscle, as well as Ca^{2+} influx across the plasma membrane using voltage- or receptor-operated channels (13, 14). The majority of released or imported Ca^{2+} in the cytosol is bound to buffer molecules, including Ca^{2+}-binding proteins (13). An essential role for the transduction of the Ca^{2+} signal is undertaken by the Ca^{2+}-binding proteins, which are characterized by the presence of a helix-loop-helix Ca^{2+}-binding motif termed EF-hand. The conformational changes of the EF-hand upon binding of Ca^{2+} can allow these proteins to interact with a range of specific binding targets and in this way regulate their function (15, 16). Ca^{2+}-binding proteins, such as human calmodulin-like protein (17), human calmodulin-like skin protein (Clsp) (18), and S100 proteins (19–21), have been characterized in the epidermis with ongoing efforts on studying their func-

* This work was supported by the Intramural Research Program of the NIAMS, National Institutes of Health. The costs of publication of this article were defrayed in part by the payment of page charges. This article must therefore be hereby marked "*advertisement*" in accordance with 18 U.S.C. Section 1734 solely to indicate this fact.

[1] To whom correspondence should be addressed: Developmental Skin Biology Unit, NIAMS, National Institutes of Health, Bldg. 50, Rm. 1525, Bethesda, MD 20892. Tel.: 301-435-7842; Fax: 301-435-7910; E-mail: morassom@mail.nih.gov.

[2] The abbreviations used are: ER, endoplasmic reticulum; Clsp, human calmodulin-like skin protein; rScarf, recombinant Scarf protein; FITC, fluorescein isothiocyanate.

tion. In previous studies, we have reported the characterization of the novel mouse skin-specific Ca^{2+}-binding proteins, Scarf (skin calmodulin-related factor), and Scarf2 (22) with their expression patterns being very similar and highly expressed in the differentiated layers of the murine epidermis (22, 23).

Here, we have examined the roles of Scarf during the epidermal differentiation process. Seven binding target proteins of Scarf were identified, and their interactions with Scarf were analyzed during epidermal barrier disruption and wound healing. We propose that Scarf plays a critical role as a Ca^{2+} sensor regulating the function of its binding target proteins in a Ca^{2+}-dependent manner during epidermal stratification and barrier recovery.

EXPERIMENTAL PROCEDURES

Scarf and Anti-Scarf Antibody Affinity Chromatography—Recombinant Scarf (rScarf) protein and purified anti-Scarf antibody were immobilized separately on *N*-hydroxysuccinimide-activated Sepharose columns according to the manufacturer's instructions (Amersham Biosciences). The coupling efficiency was 95%, calculated from the ratio of rScarf or anti-Scarf antibody in solution before and after incubation with the matrix of the column. Neonatal mouse epidermis was homogenized in a lysis buffer (10 mM Hepes, pH 7.9, 150 mM NaCl, 0.1% Triton X-100, and protease inhibitors) and then centrifuged at 10,000 × *g* for 10 min at 4 °C. After passing through a 0.22-μm filter, the Ca^{2+} concentration of the supernatants was adjusted to 2.5 mM before applying onto the columns. Elution was performed using 0.1 N glycine, and the eluted proteins were then subjected to SDS-PAGE for mass spectrometry analysis.

Mass Spectrometry—Proteins were visualized using a colloidal Coomassie Blue staining kit (Invitrogen) (24). Visible bands were excised, and proteins were digested with porcine trypsin (Promega) using a MassPREP station (Waters Associates) by a process that included extensive destaining and reduction/alkylation with iodoacetamide. After extraction from the gel pieces, the liquid samples were *in vacuo* concentrated to ~12 μl.

Liquid chromatography-coupled tandem mass spectrometry analysis was performed using a Waters CapLC system. 6.4 μl of the sample was injected onto a C-18 reverse phase trap column (Optipak Symmetry 300, Waters Associates). After 5 min, the flow was reversed through the trap column, which then coupled to a microbore high performance liquid chromatography column (VC-10-C18w-150, 5 μm, 0.15 mm × 10 cm, Micro-Tech Scientific). Solution A contained 0.2% formic acid and 1% acetonitrile, and solution B was composed of 0.2% formic acid, 1% water, and 98.8% acetonitrile. The gradient was 5% of solution B for 5 min to 35% of solution B by 15 min to 90% of solution B in 25 min. The electrospray was generated by the nebulizing nanoflow accessory, which is available with the interface at a capillary voltage of 3.5 kV. Trapping flow rates were 10 μl/min, and analytical flow rates were ~1 μl/min. Data-dependent analysis was performed with up to three parent ions of charges 2, 3, 4 in any given departure from direct mass spectrometry measurements, with time and ion count based on control of the length of tandem mass spectrometry data collection. The dynamic exclusion for 30–45 s was included to reduce ion remeasurement. Data were then processed to *.pkl files using the vendor package Masslynx (Waters Associates) with no cut off for tandem mass spectrometry data. Searches were then performed using the Mascot search engine (Center for Information Technology, National Institutes of Health).

Co-immunoprecipitation and Western Blot Analysis—Primary mouse keratinocytes were isolated from trypsinized newborn BALB/c mouse skins and lysed by repeatedly freezing and thawing in lysis buffer (10 mM Hepes, pH 7.9, 150 mM NaCl, 0.1% Triton X-100, and protease inhibitors). The lysates were centrifuged at 10,000 × *g* for 10 min at 4 °C, and supernatants were used as the cell extracts after the Ca^{2+} concentration was adjusted to 2.5 mM.

The ProFound co-immunoprecipitation kit (Pierce) was used according to the manufacturer's instructions. Briefly, each antibody (chicken anti-Scarf, mouse anti-14-3-3σ (Upstate Biotechnology), rabbit anti-14-3-3β (Upstate Biotechnology), mouse anti-annexin II (BD Biosciences), rabbit anti-annexin V (Abcam, Inc.), rabbit anti-calreticulin (Upstate Biotechnology), rabbit anti-ERp72 (Stressgen), mouse anti-nucleolin (Abcam, Inc.)) and both IgG and IgY as controls were immobilized onto biosupport medium by amine-coupling chemical reaction. Cell extracts were then incubated with each immobilized antibody for 2 h at 4 °C in the presence or absence of 10 mM EDTA. The beads were washed extensively with lysis buffer in the same conditions. Protein samples were eluted and subjected to Western blot analysis. Phosphate-buffered saline containing both 10% BLOKHen II™ (Aves Laboratories, Inc.) and 5% goat serum was used as the blocking solution to prevent nonspecific binding. The immunoreactive proteins were detected according to the enhanced chemiluminescence protocol (Pierce) using the horseradish peroxidase-linked secondary antibody (Vector Laboratories).

Epidermal Ca^{2+} Gradient Disruption—The epidermal Ca^{2+} gradient was disrupted in 8–12-week-old hairless mouse skin (from the animal laboratory of Yonsei University) while the animals were under general anesthesia with 4% chloral hydrate administered intraperitoneally and repeatedly tape-stripped on one flank with cellophane tape. The procedure was performed until the transepidermal water loss reached 40 g/m^2/h. Untreated sites on the same animals served as controls. Methods for acute barrier disruption and transepidermal water loss measurements have been reported (7, 25).

Immunofluorescence and Confocal Microscopy—Immunofluorescent staining was performed on paraffin sections of adult hairless mouse skin. The deparaffinized sections were treated with a 1:500 dilution (except for rabbit anti-filaggrin antibody, which was used at 1:2000) of the antibodies used in the co-immunoprecipitation analysis overnight at 4 °C. After washing, the sections were incubated with 1:500 dilutions of secondary antibodies for 1 h at room temperature, which included an anti-chicken fluorescein isothiocyanate (FITC)-conjugated antibody (Cappel) and an anti-rabbit or mouse rhodamine-conjugated antibody (Jackson ImmunoResearch Laboratories). The slides were mounted with Vector Shield (Vector Laboratories) and examined using laser scanning confocal microscope 510 Meta (Zeiss).

Cell Culture, Transient Transfections, and Ionomycin Treatment—Transformed PAM212 primary mouse keratinocytes were grown in Eagle's minimal essential medium supple-

mented with 10% chelex-treated fetal bovine serum (2, 22). Ca^{2+} concentration was determined by analysis in an atomic absorption spectrophotometer. Unless otherwise indicated, the Ca^{2+} concentration of the medium was adjusted to 0.05 mM to maintain a basal cell-like population of undifferentiated cells.

The open reading frame for Scarf and V5-tagged annexin V (tag at the 3′ end) were cloned into pCMV-Script (Stratagene). Keratinocytes were co-transfected using FuGENE 6 transfection reagent (Roche Applied Science) and incubated for 24 h to allow gene expression. Cells were treated with 2.5 μM ionomycin (Calbiochem) for 30 min before 4% paraformaldehyde fixation and then permeabilized with 0.2% Triton X-100 in phosphate-buffered saline. Immunofluorescence was performed with anti-Scarf and anti-V5 antibodies as described above.

Human Skin Specimens, Wounding, and Histology—Specimens of normal human skin were obtained as discarded tissue following reduction mammoplasty (approved protocol H#25121) and maintained as described previously (26). Wounds were created using 3-mm punch biopsies through the reticular dermis, and the specimens were maintained on an air-liquid interface for 4 and 7 days as previously reported (27). Each time point was collected in parallel with an unwounded skin specimen from the same donor. Samples were fixed in 10% formalin and paraffin-embedded. 7-mm skin sections were cut and stained with anti-chicken Scarf antibody (1:200) diluted in phosphate-buffered saline with 0.1% Triton X-100 (Sigma) and visualized using an anti-chicken FITC-conjugated antibody (1:250; Cappel). All sections were stained with Hoechst (Sigma) for visualization of the nucleus. All negative controls were prepared by omitting the primary antibody. The sections were analyzed using a Carl Zeiss microscope, and digital images were collected using the Adobe TWAIN_32 program.

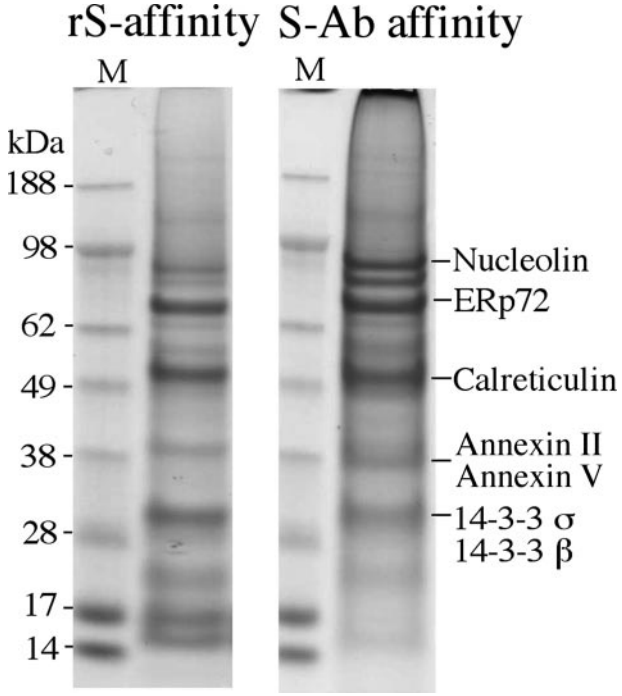

FIGURE 1. **Identification of binding target proteins interacting with Scarf by affinity chromatography and mass spectrometry.** Affinity chromatography was performed using extracts from neonatal mouse epidermis. Two affinity columns were prepared, one with recombinant Scarf protein (*rS*, *left panel*) and the other with anti-Scarf antibody (*S-Ab*, *right panel*), and eluted proteins were subjected to electrophoresis on a polyacrylamide gel. Excised bands from gel were then analyzed by mass spectrometry. Several binding target proteins, including 14-3-3σ and β, annexins II and V, calreticulin, ERp72, and nucleolin were identified.

RESULTS

Identification of Scarf-binding Target Proteins—To determine the roles of Scarf during the epidermal differentiation process, we set out to identify its binding target proteins. Recombinant Scarf (rScarf) protein and affinity-purified anti-Scarf antibody were immobilized separately on *N*-hydroxysuccinimide-activated Sepharose beads and used to capture target proteins from neonatal mouse epidermis. The eluted proteins were subjected to electrophoresis on a polyacrylamide gel, which was then stained with colloidal Coomassie Blue (Fig. 1). The identity of the bands in each preparation was determined by mass spectrometry after a trypsinization process. Binding target proteins identified in rScarf (Fig. 1, *rS*, *left panel*) or anti-Scarf antibody (*S-Ab*, *right panel*) columns were 14-3-3σ, 14-3-3β, annexin II, annexin V, calreticulin, endoplasmic reticulum protein 72 (ERp72), and nucleolin. The match score and sequence coverage (%), which indicate sequence identity between binding target proteins and trypsinized peptides from the bands of the polyacrylamide gel, are shown in Table 1. Annexin II, calreticulin, and ERp72 were marked with high match score and sequence coverage (%) in both rScarf and anti-Scarf antibody columns.

Ca^{2+} Affects Scarf-binding Target Protein Interactions—The expression of the seven Scarf-binding target proteins was corroborated in primary mouse keratinocytes by Western blot analysis (Fig. 2*A*). Cell extracts were prepared from total (*T*) and suprabasal (*S*) keratinocytes isolated by Percoll gradient from neonatal mouse skins (22). Western blot analysis with antibod-

TABLE 1

Determination of Scarf binding target proteins interacting by mass spectrometry

Data related to binding target proteins were obtained from the Mascot search engine by CIT, National Institutes of Health. rS, recombinant Scarf; S-Ab, anti-Scarf antibody; ANX II, annexin II; ANX V, annexin V; CRT, calreticulin; ERp72, Endoplasmic reticulum protein 72; NUC, nucleolin; ND, not determined.

Sample identification	Protein	Swiss-Prot accession no.	rS-affinity		S-Ab affinity	
			Match score	Sequence coverage	Match score	Sequence coverage
				%		%
1	14-3-3σ	Q9JJ20	66	11	131	14
2	14-3-3β	143B MOUSE	57	7	118	10
3	ANX II	ANX2_MOUSE	306	35	275	19
4	ANX V	AQHUP	40	3	ND	ND
5	CRT	S06763	394	35	467	38
6	ERp72	ISMSER	210	13	242	15
7	NUC	BAC38858	ND	ND	57	4

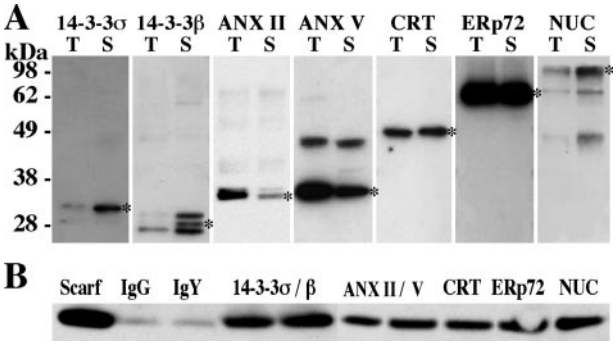

FIGURE 2. **Expression and interaction between Scarf and its binding target proteins was confirmed by Western blot and co-immunoprecipitation analysis.** *A*, equal amounts of total protein from extracts of total (*T*) and suprabasal (*S*) keratinocytes were loaded onto SDS gel, and Western blot analysis was performed with antibodies specific for each binding target protein. All binding target proteins were expressed in primary mouse keratinocytes and in the suprabasal layer of mouse epidermis. *B*, co-immunoprecipitation analyses were performed with anti-14-3-3σ, anti-14-3-3β, anti-annexin II, anti-annexin V, anti-calreticulin, anti-ERp72, and anti-nucleolin antibodies using cell extracts from primary mouse keratinocytes. Their interactions with Scarf were then confirmed by subsequent Western blot analysis with anti-Scarf antibody. Anti-IgG and anti-IgY antibodies were used as controls.

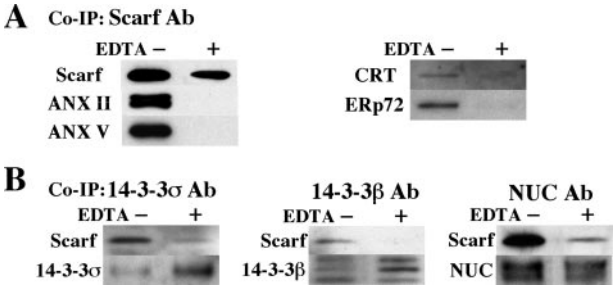

FIGURE 3. **Ca^{2+} effects on the interactions between Scarf and its binding target proteins.** The effects of Ca^{2+} on the interactions between Scarf and its binding target proteins were examined by co-immunoprecipitation analysis in the presence and absence of EDTA. *A*, co-immunoprecipitation with anti-Scarf antibody detected the interactions of Scarf with annexin II, annexin V, calreticulin, and ERp72 in the absence (−) and presence (+) of EDTA. *B*, Ca^{2+} effects on interactions with 14-3-3s and nucleolin were also visualized by co-immunoprecipitation in the absence (−) and presence (+) of EDTA. The *lower panels* for each protein demonstrates that EDTA does not have an effect on either the protein-antibody recognition itself or antibody immobilization to the co-immunoprecipitation columns.

ies specific for each binding target protein determined that all of these proteins are expressed in the differentiated layers of mouse epidermis. To verify their interaction with Scarf, co-immunoprecipitation analysis was performed with antibodies specific for 14-3-3σ, 14-3-3β, annexin II, annexin V, calreticulin, ERp72 and nucleolin, and cell extracts from primary mouse keratinocytes. Western blot with anti-Scarf antibody confirmed their interaction with Scarf (Fig. 2*B*). Anti-IgG and anti-IgY antibodies were used as negative controls.

The effect of Ca^{2+} on Scarf-binding target protein interactions was also examined by co-immunoprecipitation analysis (Fig. 3). Annexin II, annexin V, calreticulin, and ERp72 were co-immunoprecipitated with anti-Scarf antibody and visualized by Western blot using previously specified antibodies (Fig. 3*A*), whereas the interactions of 14-3-3σ, 14-3-3β and nucleolin were verified with Western blots using anti-Scarf antibody after co-immunoprecipitation with each antibody (Fig. 3*B*). All of these interactions were Ca^{2+}-dependent, because the addition of EDTA abolished or strongly diminished the binding

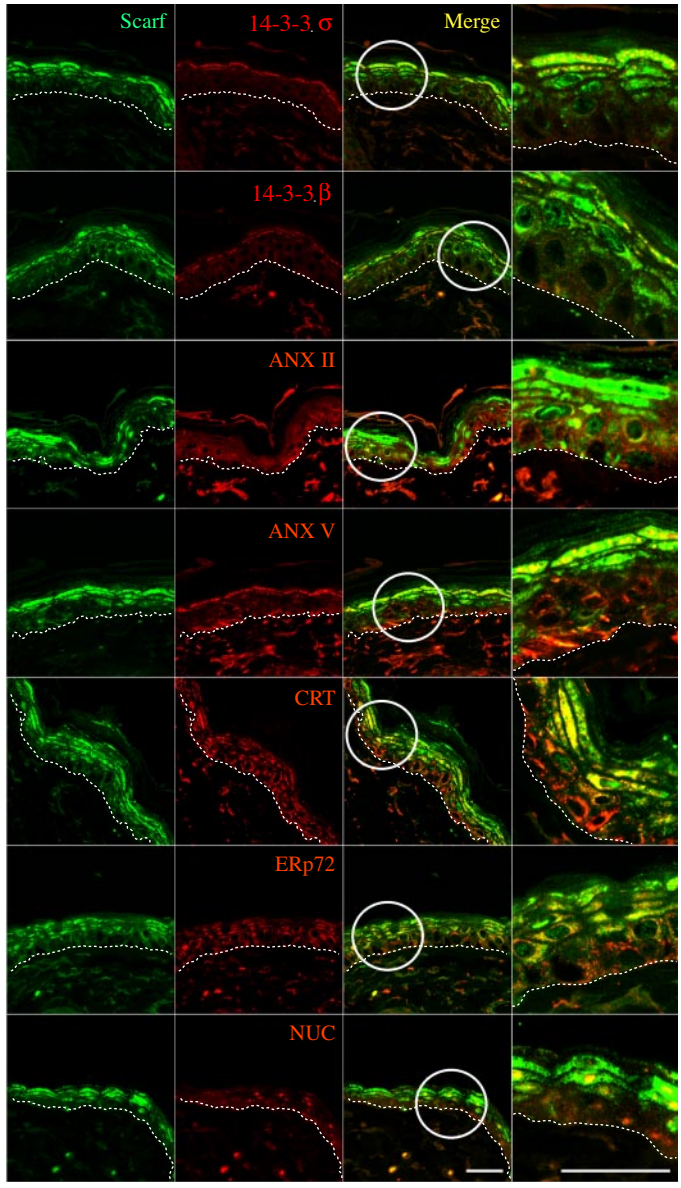

FIGURE 4. **Localization of Scarf and binding target proteins in mouse neonatal epidermis.** Scarf was detected using an anti-Scarf chicken antibody and a secondary FITC-conjugated antibody (*green*, *left panels*), and binding target proteins (14-3-3σ, 14-3-3β, annexin II, annexin V, calreticulin, ERp72 and nucleolin) were visualized using specific antibodies followed by rhodamine-conjugated secondary antibody (*red*, *middle*). Merged images are shown in the *third panels*. *Right panels* are the magnifications of the *circled areas* in the merged panels. All binding target proteins are expressed with Scarf in the differentiated layers of mouse epidermis. A *dotted line* demarcates the epidermis/dermis junction. *Scale bar*, 30 μm.

(Fig. 3). The interaction of Scarf with 14-3-3s and nucleolin could only be detected when co-immunoprecipitated with specific antibodies raising the possibility that these proteins might not bind directly to Scarf but form a complex with intermediate molecules that interact Scarf.

Localization of Binding Target Proteins and Scarf Expression—Detection of Scarf and binding target proteins was visualized in adult mouse skin sections by immunofluorescent staining and confocal microscopy (Fig. 4). Scarf was stained with FITC-conjugated secondary antibody (first panel), the binding target proteins were detected with a rhodamine-conjugated secondary

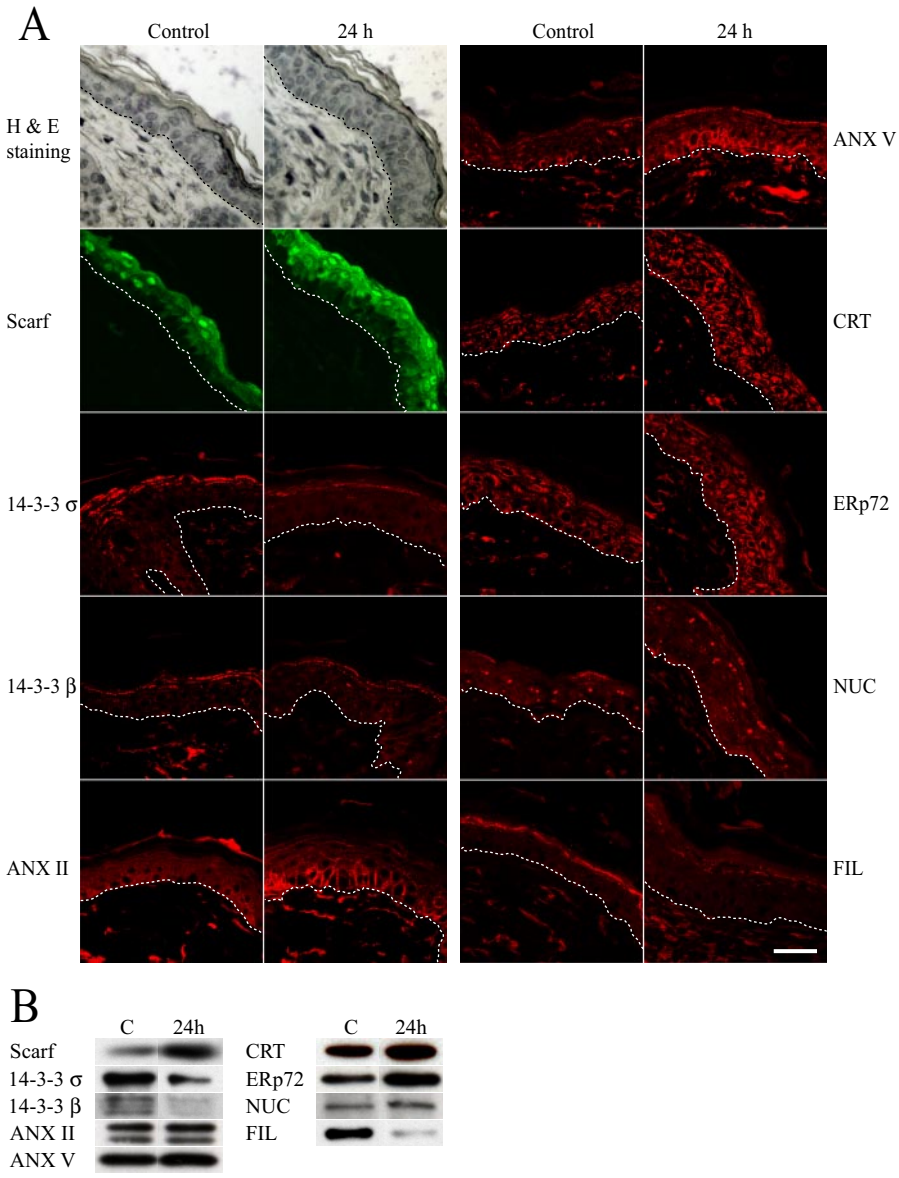

FIGURE 5. **Changes in expression patterns and levels of Scarf and its binding target proteins during acute epidermal barrier disruption.** Acute barrier disruption was performed by repeated tape stripping, and mouse skin samples were collected 24 h after treatment. Changes in expression patterns and levels of Scarf, annexin II, annexin V, calreticulin, ERp72, 14-3-3σ, 14-3-3β, and nucleolin after acute barrier disruption were detected by immunohistochemistry (*A*) and Western blot analysis (*B*). A *dotted line* demarcates the epidermis/dermis junction. *Scale bar*, 30 μm.

antibody (second panel), and the merged and magnified images appear on the third and fourth panels, respectively. The expression pattern of Scarf is consistent with previous reports (22, 23) showing that Scarf is expressed in the differentiated layers of the mouse epidermis. 14-3-3σ, 14-3-3β, and annexin V were expressed primarily in granular layers of adult mouse epidermis, whereas calreticulin, ERp72, and nucleolin were expressed throughout the adult mouse epidermis. The merged images and panel with magnified images (Fig. 4, *right panel*) show the overlap in expression of the binding target proteins with Scarf in the cytoplasm and nuclei of the epidermal, differentiated layers.

Changes in Expression Level and Localization after Alteration of Intracellular Ca^{2+} Concentration—Acute disruptions of epidermal permeability barrier function by either repeated tape stripping or acetone treatment transiently change the epidermal Ca^{2+} gradient, inducing a decrease in Ca^{2+} levels in the outer epidermis (12). To understand the possible function of Scarf and its binding target proteins in the maintenance of the epidermal Ca^{2+} gradient, we disrupted the epidermal barrier by tape stripping and collected skin samples at 3, 6, and 24 h after the disruption. The change in the expression level of Scarf and its binding target proteins was analyzed by immunohistochemistry and Western blot studies using skin sections and cell extracts of samples untreated (control) and after barrier disruption.

As shown in Fig. 5*A*, the expression level of Scarf increased in the granular layers and in the nuclei of cells in the spinous layer 24 h after acute barrier disruption. This change in expression levels is already detected in skin samples obtained 3 and 6 h after barrier disruption (data not shown), with the highest level of change visualized at 24 h after disruption (Fig. 5*A*). This result suggests that the increase in Scarf expression may precede the recovery of the epidermal Ca^{2+} gradient following the disruption. In addition, the expression level of annexin II, annexin V, calreticulin, and ERp72 are also increased 24 h after the disruption, whereas the expression levels of 14-3-3σ, 14-3-3β, and nucleolin decrease (Fig. 5). Filaggrin was used as a control, and its expression decreased in these experiments. This is consistent with previous reports that show filaggrin mRNA level decreases after acute barrier disruption and is restored after 6–24 h (12).

Distinct changes in the localization of Scarf and some of its binding target proteins were also evaluated. Fig. 6*A* shows that Scarf and annexin V are both up-regulated and become co-localized at nuclear envelopes and nuclei in the suprabasal layers of the mouse epidermis after acute barrier disruption. Translocation was also observed in transfected mouse keratinocytes. Cells co-transfected with Scarf and annexin V were treated with ionomycin to increase the intracellular Ca^{2+} concentration. In this setting, both Scarf and annexin V translocate to the nucleus after treatment with ionomycin (Fig. 6*B*). The results from these two different approaches indicate that the

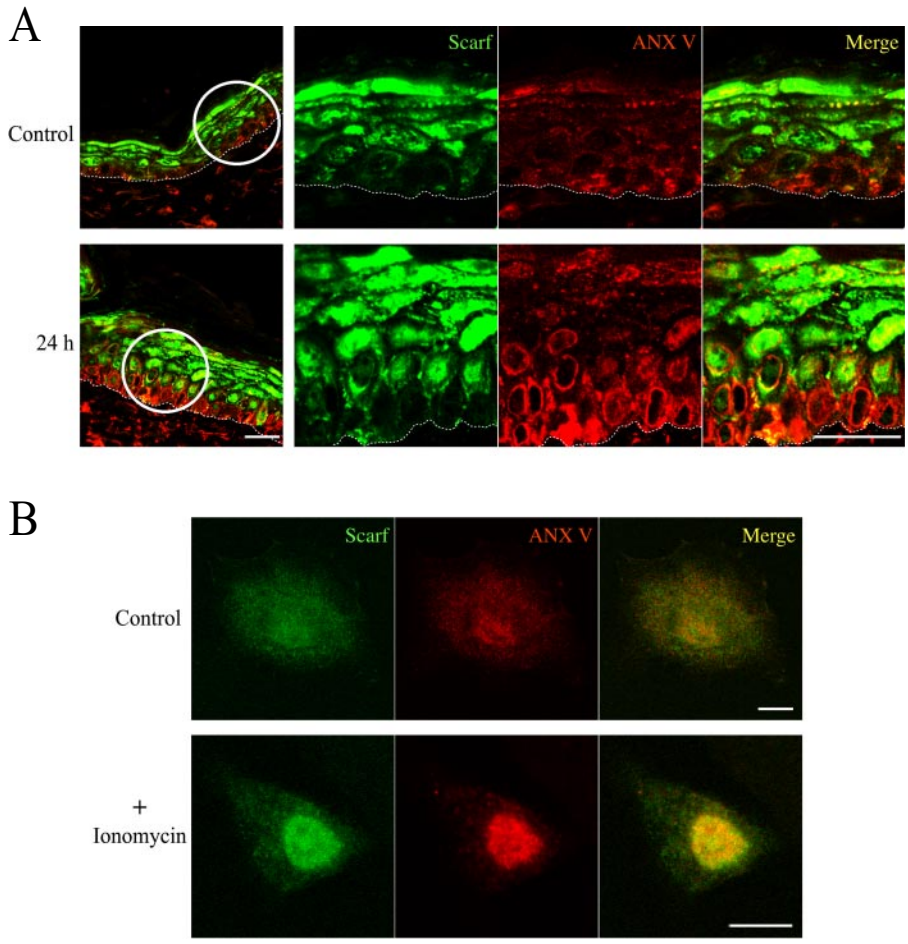

FIGURE 6. **Calcium-dependent localization of Scarf and annexin V in both barrier-disrupted skin and mouse keratinocytes.** Translocation of Scarf and annexin V was detected in after acute barrier disruption (*A*) and treatment with ionomycin to mouse keratinocytes (*B*). Scarf was stained using a secondary FITC-conjugated antibody (*green*), and annexin V was visualized by rhodamine-conjugated secondary antibody (*red*). A *dotted line* demarcates the epidermis/dermis junction. *Scale bar*, 30 μm in *A* and 10 μm in *B*.

expression of Scarf and some of its binding target proteins is up-regulated and the proteins can be relocated by changes in intracellular Ca^{2+} concentration.

Role of Scarf in Human Skin during Wound Healing—Correlation between skin injury and Ca^{2+}-binding protein function has been reported on studies with S100 proteins, which show that S100A8 and its dimerization partner, S100A9, are strongly up-regulated during wound healing, whereas their expression is very low in normal epidermis (28). We next investigated whether the Scarf human homolog, Clsp, was also up-regulated during wound repair in skin. Normal human skin was wounded by 3-mm biopsy punch and maintained at the air-liquid interface for 4, 7, and 12 days. We performed immunohistochemical analysis of the epidermis at the edge of the wounds utilizing the chicken anti-Scarf antibody that detects the human homolog Clsp (human calmodulin-like skin protein) but shows no cross-reactivity with related Ca^{2+}-binding proteins such as calmodulin or human calmodulin-like protein (22). As expected, we found Clsp/Scarf expression in the granular, differentiated layers of the unwounded human skin (18), similar to mouse epidermis (Fig. 7). Interestingly, 4 days, and even more prominently, 7 days after wounding, Clsp/Scarf expression was increased and expanded through granular and spinous layers of the epidermis (Fig. 7), similar to the epidermis after tape stripping. In addition, we found that Clsp/Scarf localizes to nuclei of the keratinocytes at 4 and 7 days post-wounding, whereas both expression and nuclear presence are restored to the base levels at 12 days post-wounding when the repair process is completed (data not shown). Taken together, we propose that Clsp/Scarf potentially participates in late stages of the wound healing process in epidermis, suggesting a role in epidermal barrier restoration.

DISCUSSION

In eukaryotic systems, Ca^{2+} ions are crucial in a variety of cellular signaling pathways. Epidermal differentiation is a Ca^{2+}-dependent process that is accompanied by increases in intracellular Ca^{2+} concentration from the proliferative basal compartment to the terminally differentiated, cornified layer of the skin (12). Ca^{2+}-dependent signaling systems respond to transient variations in Ca^{2+} concentration through members of the family of highly homologous Ca^{2+}-binding factors. These proteins function by undergoing conformational changes upon binding Ca^{2+}, which enable them to interact with specific targets and in this way modulate their function. We previously reported a novel protein Scarf characterized by the presence of four Ca^{2+}-binding EF-hand motifs, which are highly expressed in the differentiated layers of the mouse stratified epidermis (22, 23). The cell specificity of Scarf expression suggests a role in the regulation of effector proteins in Ca^{2+} signaling-dependent pathways in keratinocytes. The primary goals of this study were to determine the binding targets and putative functions of Scarf in Ca^{2+} homeostasis and epidermal differentiation.

Seven binding target proteins were identified by affinity chromatography and mass spectrometry (14-3-3σ, 14-3-3β, annexin II, annexin V, calreticulin, ERp72, and nucleolin), and their interactions with Scarf were verified by co-immunoprecipitation and co-localization studies. Recent reports have summarized the crucial roles of these proteins in diverse processes. 14-3-3s proteins are a family of seven (α/β, ϵ, η, γ, τ/θ, ζ/δ, and σ) highly conserved phosphoserine/threonine-binding factors that participate in a wide range of signaling pathways, *i.e.* signal transduction, cell cycle regulation and differentiation, apoptosis, and stress responses (29–31). Annexins are phospholipid-binding proteins that associate with membrane lipids

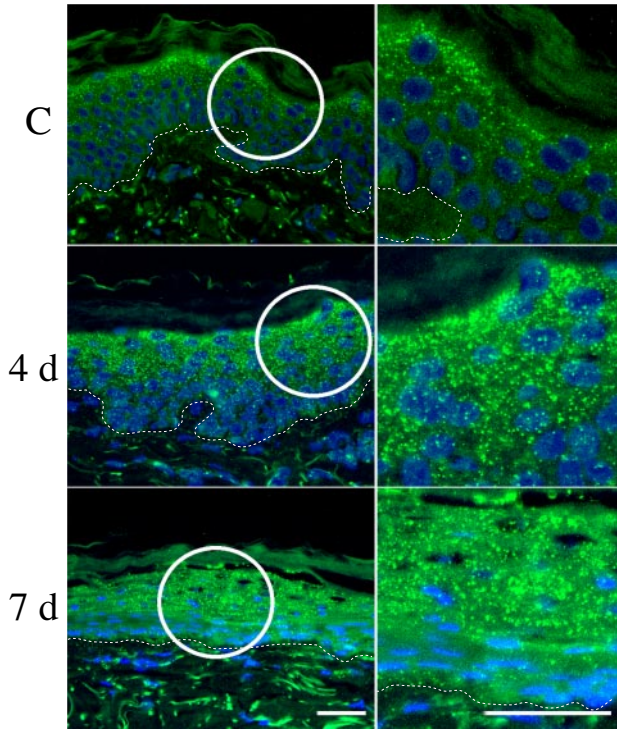

FIGURE 7. **Expression of Clsp (Scarf human homolog) in human skin during wound healing.** The expression of the Ca^{2+}-binding protein in human skin was detected using anti-Scarf antibody (*green*). The expression level increased by 7 days after skin wounding. The *right panels* are the magnifications of the *circled areas* in the *left panels*. The nuclei were visualized using Hoechst staining (*blue*). *Left panel scale bar*, 30 μm. *Right panel scale bar*, 10 μm.

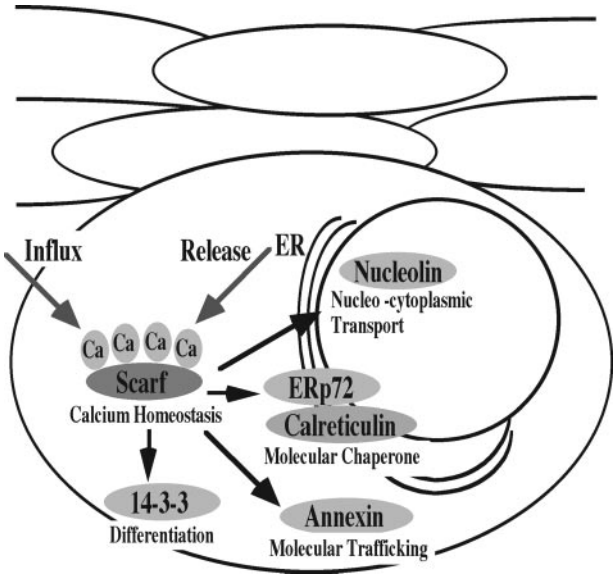

FIGURE 8. **Schematic diagram of the Scarf-mediated Ca^{2+} homeostasis in keratinocytes.** The Ca^{2+}-dependent interactions of Scarf with annexins, calreticulin, and ERp72 may play crucial roles in Ca^{2+} homeostasis, molecular trafficking, and chaperone activity, and interactions with 14-3-3σ, 14-3-3β, and nucleolin are potentially involved in growth inhibition and differentiation of keratinocytes.

in a Ca^{2+}-dependent manner and function in cellular or molecular trafficking (32). Calreticulin binds Ca^{2+} in the lumen of the ER and plays critical roles in the regulation of Ca^{2+} homeostasis (33, 34). ERp72 is one of the protein disulfide isomerases present in the ER that participates as a molecular chaperone and in protein folding (35). Nucleolin is a nuclear phosphoprotein associated with preribosomal RNA that has been implicated in the regulation of rDNA transcription and nucleocytoplasmic transport (36). The overall commonality between the Scarf-binding target proteins is that they are implicated in the regulation of cellular Ca^{2+} homeostasis at different levels and in intracellular localization, (Fig. 8) and our results demonstrate that the interaction with Scarf is Ca^{2+}-dependent (Fig. 3).

Some of the binding target proteins identified for Scarf in this study, *i.e.* annexins and nucleolin, have also been shown to interact with S100 family members. The S100 multigenic family comprises 21 Ca^{2+}-modulated proteins of the EF-hand type with intracellular and extracellular regulatory activities (19, 21). Fourteen members of this family of genes are encoded in the epidermal differentiation complex located on human chromosome 1q21, most of which are expressed in normal and/or diseased epidermis (20). Similar to what has been demonstrated for calmodulin, S100 proteins can bind to binding target proteins after undergoing conformational changes upon binding Ca^{2+}. Interactions of S100 proteins and annexins have been reported, S100A6 with annexin XI, S100A10 with annexin II, and S100A11 with annexin I (37). Furthermore, calcium-dependent co-localization at the nuclear envelope of cells was reported in the case of S100A6 and annexin XI (38). Structural and functional studies have shown that annexin II exists in cells as either a monomer or a heterotetramer complexed with S100A10 Ca^{2+}-binding protein, which participates in the Ca^{2+}-induced exocytosis of secretory granules and localizes to endosomes in the endocytic pathway (32). The formation of junctions between the lipid membrane and $[S100A10\text{-annexin II}]_2$ heterotetramer has been studied by both electron microscopy and atomic force microscopy (39, 40). Recent reports show that S100A11-annexin I also forms heterotetramers (41) that may be involved in remodeling plasma membrane structures, functions as an activated channel that mediates Ca^{2+} influx, and/or serves as a structural component of the cornified envelope (20). These activities would require a relocation of S100A11 to the cell periphery, which has been demonstrated to be dependent on Ca^{2+} and the presence of intact microtubules (42, 43). Furthermore, S100A11 has also been proposed to be a mediator of Ca^{2+}-induced growth arrest in keratinocytes through a mechanism that involves the interaction with nucleolin (44, 45). Although the specific physiological function of S100 proteins is still being studied, there is increasing evidence of their role in activities related to inflammatory processes, with several of the family members being highly up-regulated in epidermal inflammatory diseases such as psoriasis and atopic dermatitis (19, 20). It will be of great interest to evaluate whether there are similar pathways and functional roles for Scarf in these pathological conditions.

Another family of factors that has drawn much interest is the 14-3-3 proteins, which can bind in a phosphorylation-dependent fashion to important cytoplasmic and nuclear proteins and in this way prevent/promote the interactions with other proteins, modulate the activity of enzymes, sequester proteins in particular subcellular compartments, or work as adaptors to bridge two proteins (31, 46). 14-3-3s form homodimers or heterodimers that bind to the consensus motifs RS*X*pS*X*P and

R*X*(Y/F)*X*pS*X*P (*X* is any amino acid and pS is phosphoserine or phosphothreonine) present in almost all of their binding targets (31, 46). Some of the many targets reported for 14-3-3 isoforms, *i.e.* nucleolin, annexins, and 14-3-3 themselves (47, 48) were also shown to interact with Scarf. 14-3-3s have previously been implicated in human wound healing, being involved in the regulation of keratinocyte migration to the closure site (49, 50) and in the modulation of keratin filaments and mitotic progression (51). To further substantiate the important role of this family in keratinocyte biology, a recent report demonstrates that keratin 17 regulates cell growth by interaction with 14-3-3s (52). Scarf does not contain the sequence motifs for binding 14-3-3 proteins in a phosphoserine-dependent manner. However, alternative mechanisms have been recently reported for 14-3-3 interactions with β1 integrin (53). It is possible that the interaction between Scarf and 14-3-3 proteins is also achieved through a distinct motif. Alternatively, the interaction could be indirect, forming a complex with a not-yet-identified bridging protein.

Due to the established central role of Ca^{2+} in skin barrier acquisition and maintenance and to better understand the effects of change in Ca^{2+} concentration in skin on Scarf and its binding proteins, we analyzed Scarf expression after acute epidermal water barrier disruption and in wound healing. We found that Scarf expression increases after barrier disruption, indicating a potential role for Scarf in maintaining Ca^{2+} homeostasis by sensing and regulating the increase of intracellular Ca^{2+} concentration by both influx across the plasma membrane and release from the ER. Moreover, the expression level of annexin II, annexin V, calreticulin, and ERp72, which are involved in Ca^{2+}-induced exo- and endocytosis, regulation of Ca^{2+} homeostasis and protein synthesis, increases at 6 h after barrier disruption, whereas the expression of 14-3-3σ, 14-3-3β, and nucleolin, implicated in Ca^{2+}-induced growth inhibition and differentiation of keratinocytes, decreases. These results are in agreement with the report by Elias *et al.* (12) that shows decreased expression of differentiation-specific proteins while the secretion of lamellar bodies occurs simultaneously as a result of the disruption. An additional aspect studied was the calcium-dependent nuclear localization of Scarf and annexin V. Scarf and annexin V co-localized in the nucleus after increased intracellular Ca^{2+} concentration due to ionomycin treatment, re-emphasizing the crucial role of Ca^{2+} in the control of subcellular localization and the potential function of these factors. The physiological importance of this nuclear localization remains to be elucidated; however, the potential relevance is substantiated by similar nuclear translocations of annexin V, annexin XI, and 14-3-3 being found to be calcium and/or cell cycle-dependent (30, 32, 38, 52).

The second *in vivo* system utilized to study Scarf function was during wound healing. The ultimate goal of the wound healing process in epidermis is barrier restoration (54). In our human experimental model, complete closure is achieved between days 9 and 10. We found that, at day 4 of post-wounding, Clsp/Scarf is being induced, expanding through granular and spinous layers, having the highest increase at day 7. Its nuclear localization in keratinocytes at the edge of the wound indicates a plausible active role during this process. This spatiotemporal increase in Clsp/Scarf protein and its activity during wound healing in epidermis is biologically very relevant. During the early phases of wound healing, keratinocytes first migrate and subsequently proliferate to fill the gap (54). Clsp/Scarf expression was not increased during these early stages. However, we have shown that expression substantially increased at the time when keratinocytes were shifting from the activated to the differentiating state to restore the barrier. This would suggest that Clsp/Scarf plays an important role in late epidermal wound healing, perhaps participating in the change from activated to differentiating keratinocyte phenotype.

It is of immediate interest to determine how these variations in expression and/or altered interaction between Scarf and its binding target proteins translate to the maintenance of the Ca^{2+} gradient, differentiation, barrier maintenance, and wound healing and how Scarf function relates these processes to one another and the overall Ca^{2+} homeostasis of the skin.

Acknowledgments—We thank Drs. K. Zaal and E. Ralston of the NIAMS Light Imaging Section for assistance with light microscopy. We also appreciate Dr. N. Radoja, S. J. Stimpson, Y. Rivera, and Dr. O. Duverger for helpful suggestions and discussions.

REFERENCES

1. Hennings, H., Michael, D., Cheng, C., Steinert, P., Holbrook, K., and Yuspa, S. H. (1980) *Cell* **19,** 245–254
2. Dykes, P. J., Jenner, L. A., and Marks, R. (1982) *Arch. Dermatol. Res.* **273,** 225–231
3. Yuspa, S. H., Kilkenny, A. E., Steinert, P. M., and Roop, D. R. (1989) *J. Cell Biol.* **109,** 1207–1217
4. Menon, G. K., Grayson, S., and Elias, P. M. (1985) *J. Investig. Dermatol.* **84,** 508–512
5. Menon, G. K., Elias, P. M., Lee, S. H., and Feingold, K. R. (1992) *Cell Tissue Res.* **270,** 503–512
6. Mauro, T., Bench, G., Sidderas-Haddad, E., Feingold, K. R., Elias, P. M., and Cullander, C. (1998) *J. Investig. Dermatol.* **111,** 1198–1201
7. Menon, G. K., Feingold, K. R., and Elias, P. M. (1992) *J. Investig. Dermatol.* **98,** 279–289
8. Grubauer, G., Feingold, K. R., and Elias, P. M. (1987) *J. Lipid Res.* **28,** 746–752
9. Feingold, K. R., Man, M. Q., Menon, G. K., Cho, S. S., Brown, B. E., and Elias, P. M. (1990) *J. Clin. Investig.* **86,** 1738–1745
10. Holleran, W. M., Man, M. Q., Gao, W. N., Menon, G. K., Elias, P. M., and Feingold, K. R. (1991) *J. Clin. Investig.* **88,** 1338–1345
11. Proksch, E., Feingold, K. R., Man, M. Q., and Elias, P. M. (1991) *J. Clin. Investig.* **87,** 1668–1673
12. Elias, P. M., Ahn, S. K., Denda, M., Brown, B. E., Crumrine, D., Kimutai, L. K., Komuves, L., Lee, S. H., and Feingold, K. R. (2002) *J. Investig. Dermatol.* **119,** 1128–1136
13. Woodard, G. E., and Rosado, J. A. (2005) *Curr. Top. Dev. Biol.* **65,** 189–210
14. Berridge, M. J., Bootman, M. D., and Roderick, H. L. (2003) *Nat. Rev. Mol. Cell. Biol.* **4,** 517–529
15. Nelson, M. R., and Chazin, W. J. (1998) *Protein Sci.* **7,** 270–282
16. Lewit-Bentley, A., and Rety, S. (2000) *Curr. Opin. Struct. Biol.* **10,** 637–643
17. Rogers, M. S., Kobayashi, T., Pittelkow, M. R., and Strehler, E. E. (2001) *Exp. Cell Res.* **267,** 216–224
18. Mehul, B., Bernard, D., Simonetti, L., Bernard, M. A., and Schmidt, R. (2000) *J. Biol. Chem.* **275,** 12841–12847
19. Heizmann, C. W., Fritz, G., and Schafer, B. W. (2002) *Front. Biosci.* **7,** 1356–1368
20. Eckert, R. L., Broome, A. M., Ruse, M., Robinson, N., Ryan, D., and Lee, K. (2004) *J. Investig. Dermatol.* **123,** 23–33
21. Donato, R. (2003) *Microsc. Res. Tech.* **60,** 540–551
22. Hwang, M., and Morasso, M. I. (2003) *J. Biol. Chem.* **278,** 47827–47833

23. Hwang, M., Kalinin, A., and Morasso, M. I. (2005) *Gene Expr. Patterns* **5,** 801–808
24. Perkins, D. N., Pappin, D. J., Creasy, D. M., and Cottrell, J. S. (1999) *Electrophoresis* **20,** 3551–3567
25. Grubauer, G., Elias, P. M., and Feingold, K. R. (1989) *J. Lipid Res.* **30,** 323–333
26. Lee, B., Vouthounis, C., Stojadinovic, O., Brem, H., Im, M., and Tomic-Canic, M. (2005) *J. Mol. Biol.* **345,** 1083–1097
27. Stojadinovic, O., Brem, H., Vouthounis, C., Lee, B., Fallon, J., Stallcup, M., Merchant, A., Galiano, R. D., and Tomic-Canic, M. (2005) *Am. J. Pathol.* **167,** 59–69
28. Thorey, I. S., Roth, J., Regenbogen, J., Halle, J. P., Bittner, M., Vogl, T., Kaesler, S., Bugnon, P., Reitmaier, B., Durka, S., Graf, A., Wockner, M., Rieger, N., Konstantinow, A., Wolf, E., Goppelt, A., and Werner, S. (2001) *J. Biol. Chem.* **276,** 35818–35825
29. Darling, D. L., Yingling, J., and Wynshaw-Boris, A. (2005) *Curr. Top. Dev. Biol.* **68,** 281–315
30. Tzivion, G., and Avruch, J. (2002) *J. Biol. Chem.* **277,** 3061–3064
31. Mhawech, P. (2005) *Cell Res.* **15,** 228–236
32. Gerke, V., Creutz, C. E., and Moss, S. E. (2005) *Nat. Rev. Mol. Cell. Biol.* **6,** 449–461
33. Gelebart, P., Opas, M., and Michalak, M. (2005) *Int. J. Biochem. Cell Biol.* **37,** 260–266
34. Michalak, M., Robert Parker, J. M., and Opas, M. (2002) *Cell Calcium* **32,** 269–278
35. Jessop, C. E., Chakravarthi, S., Watkins, R. H., and Bulleid, N. J. (2004) *Biochem. Soc. Trans.* **32,** 655–658
36. Ginisty, H., Sicard, H., Roger, B., and Bouvet, P. (1999) *J. Cell Sci.* **112,** 761–772
37. Gerke, V., and Moss, S. E. (1997) *Biochim. Biophys. Acta* **1357,** 129–154
38. Tomas, A., and Moss, S. E. (2003) *J. Biol. Chem.* **278,** 20210–20216
39. Lambert, O., Gerke, V., Bader, M. F., Porte, F., and Brisson, A. (1997) *J. Mol. Biol.* **272,** 42–55
40. Menke, M., Gerke, V., and Steinem, C. (2005) *Biochemistry* **44,** 15296–15303
41. Rety, S., Osterloh, D., Arie, J.-P., Tabaries, S., Seeman, J., Russo-Marie, F., Gerke, V., and Lewit-Bentley, A. (2000) *Structure* **8,** 175–184
42. Broome, A. M., Ryan, D., and Eckert, R. L. (2003) *J. Histochem. Cytochem.* **51,** 675–685
43. Broome, A. M., and Eckert, R. L. (2004) *J. Investig. Dermatol* **122,** 29–38
44. Sakaguchi, M., Miyazaki, M., Takaishi, M., Sakaguchi, Y., Makino, E., Kataoka, N., Yamada, H., Namba, M., and Huh, N. H. (2003) *J. Cell Biol.* **163,** 825–835
45. Sakaguchi, M., Miyazaki, M., Sonegawa, H., Kashiwagi, M., Ohba, M., Kuroki, T., Namba, M., and Huh, N. H. (2004) *J. Cell Biol.* **164,** 979–984
46. Hermeking, H. (2003) *Nat. Rev. Cancer* **3,** 931–943
47. Pozuelo Rubio, M., Geraghty, K. M., Wong, B. H. C., Wood, N. T., Campbell, D. G., Morrice, N., and Mackintosh, N. (2004) *Biochem. J.* **379,** 395–408
48. Jin, J., Smith, F. D., Stark, C., Wells, C. D., Fawcett, J. P., Kulkarni, S., Metalnikov, P., O'Donnell, P., Taylor, P., Taylor, L., Zougman, A., Woodgett, J. R., Langeberg, L. K., Scott, J. D., and Pawson, T. (2004) *Curr. Biol.* **14,** 1436–1450
49. Santoro, M. M., Gaudino, G., and Marchisio, P. C. (2003) *Dev. Cell* **5,** 257–271
50. Ghahary, A., Marcoux, Y., Karimi-Busheri, F., Li, Y., Tredget, E. E., Kilani, R. T., Lam, E., and Weinfeld, M. (2005) *J. Investig. Dermatol.* **124,** 170–177
51. Ku, N.-O., Michie, S., Resurreccion, E. Z., Broome, R. L., and Omary, M. B. (2002) *Proc. Natl. Acad. Sci. U. S. A.* **99,** 4373–4378
52. Kim, S., Wong, P., and Coulombe, P. A. (2006) *Nature* **441,** 362–365
53. Rodriguez, L. G., and Guan, J.-L. (2005) *J. Cell. Physiol.* **202,** 285–294
54. Morasso, M. I., and Tomic-Canic, M. (2005) *Biol. Cell* **97,** 173–183